Intrinsic free carrier mobility of quantum wells in polar materials

J-L. Farvacque and F. Carosella
Laboratoire de Structure et Propriétés de l'Etat Solide, CNRS, UMR 8008, Université des Sciences et Technologies de Lille, 59655 Villeneuve d'Ascq Cedex, France

(Received 8 July 2004; revised manuscript received 19 May 2005; published 29 September 2005)

The intrinsic mobility of AlGaN/GaN quantum wells is numerically computed, assuming that it results from the free carrier scattering by the natural plasmon and/or phonon hybrid modes initially introduced by Varga and which self-consistently issue from the full dielectric response of the material. We first develop a physical approach (i) which allows us to find back in a simple way the transition probability which was initially obtained for three-dimensional systems by Kim *et al.* in the frame of the second quantization formalism and (ii) which allows us to easily extend this formalism to the case of multi subband quantum wells. Then, the full two-dimensional dielectric function and its corresponding scattering potential is numerically computed, allowing us to predict the order of magnitude that can be expected for the low-field intrinsic mobility versus free carrier density in triangular quantum wells. We finally compare this scattering mechanism with the usual extrinsic scattering mechanisms associated with impurities, dislocations, and interface roughness.

DOI: 10.1103/PhysRevB.72.125344 PACS number(s): 72.10.Bg

I. INTRODUCTION

AlGaN/GaN heterostructures have been subjected to a lot of experimental and theoretical studies since they offer a unique situation where, due to the spontaneous polarization discontinuity at the heterostructure (0,0,0,1) interface and also to the piezoelectric polarization that appears in the strained AlGaN layer, the interface plane bears a strong positive charge and, as a consequence, attracts free electrons that form a two-dimensional electron gas (2DEG), without the need of any external doping.[1–6] The total interface polarization charge is so large that one currently obtains 2D electron gas with an areal electron density that can reach more than 2×10^{13} cm^{-2}. In these circumstances, such quantum wells are expected to have a large conductivity with good carrier mobility (lack of impurity scattering) and are considered as good candidates for power device applications. However, in the current state of the art for the epitaxial heterostructure growth of such 2D electron gas, the carrier mobility has shown to be a strongly decreasing function of the carrier density.[7] Such a behavior could be theoretically explained in Refs. 8 and 9 in the following terms: in order to obtain large polarization discontinuity effects and large piezoelectric polarizations, one must use increasing Al compositions x of the ternary $Al_xGa_{1-x}N$ cap layer as well as increasing thickness of the AlGaN cap layer. This being done, the subsequent lattice mismatch between the AlGaN cap layer and the bulk GaN substrate increases. Thus, a higher elastic energy is stored in the cap layer with increasing x compositions and/or increasing cap layer thickness. As soon as a critical elastic energy is reached in the AlGaN cap layer, the material is then subjected to strain relaxation mechanisms which unavoidably induce the appearance of defects such as dislocation tangles, surface cracks, alloy reordering, etc. Such defects lead to a spatial modification of the strain field as well as of the spontaneous polarization. Consequently, the strain relaxation mechanisms, occurring when large carrier densities are wanted, induce a spatial dependent interface charge which was called "interface electrical roughness" in Ref. 9. It was shown that this interface electrical roughness strongly decreases the carrier mobility.

Obviously, the AlGaN/GaN epitaxial growth is in permanent progress and daily new mobility records can be found in literature that overcome the mean results which were published in Ref. 9. At the time this paper was written, a room temperature mobility of about 2000 cm^2/Vs could be obtained at a carrier density of 8×10^{12} cm^{-2} (Ref. 10) or again 1500 cm^2/Vs at a carrier density of $2.15\ 10^{13}$ cm^{-2} (Ref. 11). Thus, the question is less being able to explain the bad carrier mobility that is currently obtained, but more to predict the order of magnitude of the maximum mobility that we may expect in perfect AlGaN/GaN quantum wells which would only be submitted to the intrinsic scattering mechanisms.

Intrinsic scattering mechanisms are essentially connected to acoustic and optical phonons. However, similarly to the electron-hole scattering mechanisms, direct electron-electron interactions have frequently been considered as an intrinsic effective scattering mechanism. Such mechanisms were initially introduced as a possible explanation of the residual resistivity of metals at very low temperature.[12–14] However, it has been quickly recognized that the carrier-carrier interaction cannot constitute by itself a relaxation process as the other usual scattering centers (impurities, phonons) can, since, during a two-particles collision, the whole momentum as well as the energy are conserved. Thus, the carrier-carrier interaction manifests only through the modifications it brings to the other scattering mechanisms[15–19] and, for instance, through its dynamical dielectric response.

Generally speaking, the full dielectric response of any material is made of a lattice contribution and an electronic contribution. In polar materials, the lattice dielectric function is given by Refs. 20 and 21 as follows:

$$\varepsilon_L(\omega)=\varepsilon_\infty\frac{\omega_{LO}^2-\omega(\omega-i\gamma)}{\omega_{TO}^2-\omega(\omega-i\gamma)}, \tag{1.1}$$

where ω_{LO} and ω_{TO} are the longitudinal and transverse optical phonons frequencies. γ is a damping frequency related to

the phonon lifetime $\tau_{ph} \sim 1/\gamma$. Notice that, in the undamped case ($\gamma=0$), the zeros and poles of the dielectric response correspond to natural vibration modes of the material, here: the longitudinal and transverses optical modes. The electronic dielectric contributions are given by the Lindhard dielectric function[22] which, for a three-dimensional (3D) system, is

$$\varepsilon_e(q,\omega) = 1 - \frac{e^2}{\varepsilon_0 q^2} \sum_{k,k'} \frac{(f_{k'} - f_k)|\langle k|e^{-iqr}|k'\rangle|^2}{\varepsilon_{k'} - \varepsilon_k - \omega + i\alpha} = 1 - \chi_e(q,\omega), \tag{1.2}$$

where f_k is the equilibrium Fermi-Dirac occupation function. In the Lindhard derivation, α is an infinitely small positive number. In the particular case of metals and the small q limit, it is standard to show that expression (1.2) reduces to

$$\varepsilon_e(\omega) = 1 - \frac{ne^2}{m\varepsilon_0\omega^2} = 1 - \frac{\omega_p^2}{\omega^2}, \tag{1.3}$$

whose zeros correspond to the usual plasmon modes. Such plasmon modes also exist for semiconductors. Considering the full material dielectric response given by

$$\varepsilon_T(q,\omega) = \varepsilon_L(\omega) - \chi_e(q,\omega), \tag{1.4}$$

Varga[23] was the first to point out that its zeros were natural vibration modes associated with hybrid phonon and/or plasmon boson particles, which should be considered self-consistently as the intrinsic scattering centers. The transition probability $W(k,k')$ associated with such particles and, therefore, with the self-consistent response of the material was calculated in the case of 3D systems in the pioneer work of Kim *et al.*[24] and is given by

$$W(k,k') = \frac{e^2}{V\varepsilon_0 q^2}\delta_{k',kq}\int_{-\infty}^{\infty} \mathrm{Im}\left(\frac{N(\omega)+1/2\pm 1/2}{\varepsilon_T(q,\omega)}\right) \times \delta(\varepsilon_{k'} - \varepsilon_k \pm \omega)d\omega, \tag{1.5}$$

where $N(\omega)$ is the Bose-Einstein statistics and k and k' are free electronic states. The aim of this paper is to derive the corresponding expression in the case of a 2D multisubband electronic system in view to calculate the intrinsic mobility that may be expected in AlGaN/GaN quantum wells.

II. THE INTRINSIC TRANSITION PROBABILITY

A. A simple way to recover the 3D Kim's formulation

Expression (1.5) was obtained using a very heavy derivation based on the use of the second quantization formalism. Although such a development should also be done in the 2DEG case, it would lead to very tedious steps. Instead, we present physical but very simple arguments allowing us to find back Eq. (1.5) and then to find a simple way to adapt it to the 2D case. Note that our intuitive development can simply be considered as a physical interpretation of the Kim *et al.* derivation. For doing this, we consider an elementary charge distribution moving with a velocity $\mathbf{v}$ through a 3D dielectric medium and whose density is $\rho^{ext}(r,t) = e\delta(r - \mathbf{v}t)$, leading to an elementary current density $j = \rho\mathbf{v}$. The charge density Fourier transform is

$$\rho^{ext}(q,\omega') = e2\pi\delta(\omega' - q\mathbf{v}) = e2\pi\delta(\omega' - \omega), \tag{2.1}$$

where we have defined the angular frequency $\omega = q\mathbf{v}$ characterizing the moving particle. This perturbation is responsible for the appearance of an induced electric field $E^{ind}(r,t)$ due to the dielectric medium response. The time average of the power density jE^{ind} lost by the moving particle through this induced field is given by

$$\langle jE^{ind}\rangle_{time} = \lim_{T\to\infty} \frac{1}{T}\int_{-T/2}^{T/2} \rho^{ext}(r,t)\mathbf{v}E^{ind}(r,t)dt. \tag{2.2}$$

In the following, we will omit the symbol "lim" for simplifying the notations. Expression (2.2) may also be given in terms of time Fourier transforms, which leads to

$$\langle jE^{ind}\rangle_{time} = \frac{1}{T(2\pi)}\int \rho^{ext}(r,-\omega')vE^{ind}(r,\omega')d\omega'. \tag{2.3}$$

The expected value of the power loss density calculated for any k state is

$$\langle k|jE^{ind}|k\rangle = \frac{1}{T(2\pi)}\int \sum_{k'} \langle k|\rho^{ext}(r,-\omega')|k'\rangle \times \langle k'|vE^{ind}(r,\omega')|k\rangle d\omega'. \tag{2.4}$$

Transforming the integral over ω' into a sum and making the variable change $\omega' = \omega_{k'} - \omega_k = \omega_{k'k}$ we have

$$\langle k|jE^{ind}d|k\rangle = \sum_{k',\omega_{k'k}} \frac{1}{T^2}\langle k|\rho^{ext}(r,-\omega_{k'k})|k'\rangle\langle k'|vE^{ind}(r,\omega_{k'k})|k\rangle. \tag{2.5}$$

Introducing spatial Fourier transforms of Maxwell equations and making use of the dielectric function $\varepsilon(q,\omega)$ of the medium, the induced field may be written

$$E^{\mathrm{ind}}(q,\omega') = -iqV^{\mathrm{ind}}(q,\omega') = -iqV^{\mathrm{ext}}(q,\omega')\left(\frac{1}{\varepsilon(q,\omega')}-1\right) = -iq\frac{\rho^{\mathrm{ext}}(q,\omega')}{\varepsilon_0 q^2}\left(\frac{1}{\varepsilon(q,\omega')}-1\right). \quad (2.6)$$

Using (2.6), the nonvanishing real part of Eq. (2.4) is given by

$$\langle k|jE^{\mathrm{ind}}|k\rangle = \frac{1}{T^2V^2}\sum_{k',\omega_{k'k}}\frac{|\rho^{\mathrm{ext}}(q,\omega_{k'k})|^2}{\varepsilon_0 q^2}qv\,\mathrm{Im}\left(\frac{1}{\varepsilon(q,\omega_{k'k})}\right)|\langle k|e^{-iqr}|k'\rangle|^2. \quad (2.7)$$

This last expression shows that the time averaged power density expected value for any k state is the result of k to k' transitions which correspond each to the exchange of energy quanta $\omega_{k'k}$ with the time probability $W(k,k')$. For the whole crystal of volume V, considering (2.1), the probability per unit time is then given by

$$W(k,k',\omega) = \frac{4\pi^2}{T^2V}\frac{e^2}{\varepsilon_0 q^2}\,\mathrm{Im}\left(\frac{1}{\varepsilon(q,\omega_{k'k})}\right)|\langle k|e^{-iqr}|k'\rangle|^2 \times\delta^2(\omega_{k'k}-\omega). \quad (2.8)$$

Since the imaginary part of the inverse dielectric function is maximum when its real part vanishes, the transition probabilities expressed by (2.8) are due to the natural vibrations of the material corresponding to hybrid phonon and/or plasmon particles. Thus, to get a final formula, it is also necessary to distinguish between the absorption and emission process and to weight formula (2.9) by the corresponding Bose-Einstein statistics. Finally, integrating over the whole frequency range and setting one of the two Dirac functions to the value $\delta(\omega=0)=T/2\pi$, we obtain the intrinsic transition probability given by

$$W^{\pm}(k,k') = \frac{1}{V}\frac{e^2|\langle k|e^{iqr}|k'\rangle|^2}{\varepsilon_0 q^2}\int_{-\infty}^{\infty}\mathrm{Im}\left(\frac{N(\omega)+1/2\pm1/2}{\varepsilon(q,\omega)}\right)\times\delta(\varepsilon_{k'}-\varepsilon_k\pm\omega)d(\omega) \quad (2.9)$$

as previously found in Ref. 24.

B. Case of two-dimensional multisubband systems

We now consider a 2D system whose subbands are characterized by a series of envelop functions $Z_n(z)$. Such a system is disturbed by an incoming particle moving with a velocity $\mathbf{v}$ within the 2D Oxy plane. Its density is of the form $\rho^{\mathrm{ext}}(\mathbf{r},z,t)=e\delta(\mathbf{r}-\mathbf{v}t)\delta(z-z_0)$ where $\mathbf{r}$ is now a 2D vector and z_0 a particular position along the Oz axis of the quantum well. Its Fourier transform is then

$$\rho^{\mathrm{ext}}(q,q_z,\omega') = e2\pi\delta(\omega'-q\mathbf{v})e^{iq_zz_0} = e2\pi\delta(\omega'-\omega)e^{iq_zz_0}, \quad (2.10)$$

where we have introduced the angular frequency $\omega=q\mathbf{v}$ characterizing the moving particle in the 2D plane. Following the steps introduced in Sec. II A, the power density matrix element expected value calculated for any $|n,k\rangle$ state is now given by

$$\langle n,k|jE^{\mathrm{ind}}|n,k\rangle = \frac{1}{T^2(2\pi)^6}\sum_{n',k',\omega_{k'k}}\int\rho^{\mathrm{ext}}(q',q'_z,-\omega_{k'k})\mathbf{v}E^{\mathrm{ind}}(q,q_z,\omega_{k'k}) \times\langle n,k|e^{-i(q'\mathbf{r}'+q'_zz')}|n',k'\rangle \times\langle n',k'|e^{-i(q)\mathbf{r}+q_zz}|n,k\rangle d^2q'd^2qdq'_zdq_z. \quad (2.11)$$

The matrix elements appearing in (2.11) are

$$\langle n,k|e^{-i(q\mathbf{r}+q_zz)}|n',k'\rangle = \delta_{k',k+q}\int Z_n^*(z)Z_{n'}(z)e^{-iq_zz}dz = \delta_{k',k+q}G_{n,n'}(q_z). \quad (2.12)$$

The above expression (2.12) also defines the function $G_{nn'}(q_z)$. Thus, the $|n,k\rangle$ state expected value of the power density is

$$\langle n,k|jE^{\mathrm{ind}}|n,k\rangle = \sum_{n'k',\omega_{k'k}}\frac{\delta_{k',k+q}}{T^2S^2(2\pi)^2}\int\rho^{\mathrm{ext}}(-q,q'_z,-\omega_{k'k}) \times\mathbf{v}E^{\mathrm{ind}}(q,q_z,\omega_{k'k})G_{n,n'}(q'_z)G_{n'n}(q_z)dq'_zdq_z. \quad (2.13)$$

Introducing the notation

$$F_{n,n'}(q,\omega) = \frac{1}{2\pi}\int G_{n,n'}(q_z)F(q,q_z,\omega)dq_z, \quad (2.14)$$

expression (2.13) becomes

$$\langle n,k|jE^{\mathrm{ind}}|n,k\rangle = \sum_{n',k',\omega_{k'k}} -i\frac{\delta_{k'k+q}}{T^2S^2}\rho^{\mathrm{ext}^*}_{n',n}(q,\omega_{k'k})\mathbf{v}qV^{\mathrm{ind}}_{n'n}(q,\omega_{k'k}). \quad (2.15)$$

In a 2D system, owing to the lack of translation invariance along the Oz axis and to the presence of several subbands, it is no more possible to describe the electronic dielectric response by a single function. Instead, it was shown in Ref. 25 that a dielectric function tensor must be introduced so that

$$\sum_{n,n'}\varepsilon^{n,n'}_{m,m'}(q,\omega)V^{\mathrm{tot}}_{n,n'}(q,\omega) = V^{\mathrm{ext}}_{m,m'}(q,\omega), \quad (2.16)$$

where $V^{\mathrm{tot}}_{n,n'}(q,\omega)$ and $V^{\mathrm{ext}}_{m,m'}(q,\omega)$ are defined as in (2.14) and where the dielectric tensor matrix elements are given by

$$\varepsilon^{n,n'}_{m,m'}(q,\omega) = \varepsilon_L(\omega)\delta^n_m\delta^{n'}_{m'} - \frac{e^2}{\varepsilon_0}\sum_{q_z}\frac{G_{m,m'}(q_z)G^*_{n,n'}(q_z)}{(q^2+q_z^2)}\chi^e_{n,n'}(q,\omega) \tag{2.17}$$

with

$$\chi^e_{n,n'}(q,\omega) = \sum_k \frac{f_{n',k+q}-f_{n,k}}{\varepsilon_{n',k+q}-\varepsilon_{n,k}-\omega+i\alpha}. \tag{2.18}$$

The dielectric function tensor may be easily reversed numerically owing to the finite number of subbands. Thus, introducing the reversed dielectric tensor, we obtain

$$V^{\text{ind}}_{n'n}(q,\omega) = \sum_{n,n'}[\varepsilon^{-1}(q,\omega)]^{m',m}_{n',n}V^{\text{ext}}_{m',m}(q,\omega) - V^{\text{ext}}_{n',n}(q,\omega). \tag{2.19}$$

Since the incoming charge does not work in its own field, after having retained the real nonvanishing part only, the matrix element (2.15) becomes

$$\langle n,k|jE^{\text{ind}}|n,k\rangle = \sum_{n',k',\omega_{k'k}}\frac{\delta_{k',k+q}}{T^2S^2} \times \text{Im}\left\{\rho^{\text{ext}*}_{n',n}(q,\omega_{k'k})\mathbf{v}q\sum_{m,m'}(\varepsilon^{-1})^{m',m}_{n',n}V^{\text{ext}}_{m'm}(q,\omega_{k'k})\right\}. \tag{2.20}$$

Using (2.10) and following the same development as in Sec. II A, we deduce the following transition probability

$$W^{\pm}(n,k,n',k') = \frac{L}{S}\frac{e^2\delta_{k'kq}}{\varepsilon_0}\,\text{Im}\sum_{m,m'}\int\frac{G^*_{n',n}(q'_z)G_{m',m}(q_z)e^{i(q_z-q'_z)z_0}}{q^2+q_z^2}dq_z dq'_z \times\int_{-\infty}^{\infty}[\varepsilon^{-1}(q,\omega)]^{m',m}_{n',n}\left(N(\omega)+\frac{1}{2}\pm\frac{1}{2}\right)\delta(\varepsilon_{k'}-\varepsilon_k\pm\omega)d(\omega). \tag{2.21}$$

The remaining parameter z_0 is arbitrarily chosen as the z position at which the electronic density is maximum in the quantum well. Expression (2.21) constitutes the straightforward extension of the 3D transition probability to the case of a multisubband 2D system. The complexity of (2.21) prevents any simple comparison with the formula proposed in Ref. 26 and straightforwardly deduced from the 3D Kim's result in the case of a single subband quantum well without any justification.

III. THE LINEARIZED BOLTZMANN EQUATION

A. The relaxation time

Restricting the present derivation to the case of an external electric force $F=eE$ only, the Boltzmann kinetic equation for a given $|n,k\rangle$ state and a given spin leads to Ref. 9

$$\left(\frac{\partial f_{n,k}}{\partial t}\right)_{\text{coll}} = \frac{\partial f_0}{\partial\varepsilon_{n,k}}\mathbf{v}_{n,k}F. \tag{3.1}$$

The collision term results from the simultaneous action of the various elastic scattering mechanisms that are present in the material (impurities, dislocations, acoustic phonons, etc.) and of the hybrid optical phonon and/or plasmon interaction. The first class of scattering mechanisms are in the following represented by the transition probability $W^{\text{elas}}_{n,n'}(k,k') = W^{\text{elas}}_{n',n}(k',k)$, while for the second class we separate explicitly the emission and absorption processes. The time variation of a k state occupation function due to collisions is then obtained by weighting the transition probabilities by the occupation rate f_{nk} of the initial state and the empty occupation rate $1-f_{nk}$ of the final state, by writing $f_{nk}=f_{0nk}+\delta f_{nk}$ and keeping first-order terms. This leads to

$$\left(\frac{\partial f_{nk}}{\partial t}\right)_{\text{coll}} = -\delta f_{nk}\sum_{n'k'}\{W^{\text{elas}}_{n,n'}(k,k') + [W^{+}_{n,n'}(k,k') + W^{-}_{n,n'}(k,k')](1-f_{0n'k'}) + [W^{+}_{n',n}(k',k) + W^{-}_{n',n}(k',k)]f_{0n'k'}\} + \sum_{n',k'}\{W^{\text{elas}}_{n,n'}(k,k') + [W^{+}_{n,n'}(k,k') + W^{-}_{n',n}(k',k)]f_{0nk} + [W^{+}_{n',n}(k',k) + W^{-}_{n',n}(k',k)](1-f_{0nk})\}\delta f_{n'k'}. \tag{3.2}$$

We define

$$\frac{1}{\tau^0_{n,k}} = \sum_{n'k'} W^{\text{elas}}_{n,n'}(k,k') + [W^{+}_{n',n}(k,k') + W^{-}_{n',n}(k,k')]f_{0n'k'} + [W^{+}_{n,n'}(k,k') + W^{-}_{n,n'}(k,k')](1-f_{0n'k'}) \tag{3.3}$$

and

$$G_{n,n'}(k,k') = W^{\text{elas}}_{n,n'}(k,k') + [W^{+}_{n,n'}(k,k') + W^{-}_{n,n'}(k,k')]f_{0nk} + [W^{+}_{n',n}(k',k) + W^{-}_{n',n}(k',k)](1-f_{0nk}). \tag{3.4}$$

With such notations, Eq. (3.1) leads to

$$\delta f_{nk} = -\frac{\partial f_{0,nk}}{\partial \varepsilon_{nk}} \mathbf{v}_k F \tau_{n,k}, \tag{3.5}$$

where, in the case of isotropic scattering centers

$$\tau_n(\varepsilon_k) = \tau^0_n(\varepsilon_k)\left(1 + \sum_{n'k'} G_{n,n'}(k,k')\frac{f_{0,n'k'}(1-f_{0,n'k'})}{f_{0,nk}(1-f_{0,nk})}\frac{k'}{k} \times \cos(k,k')\tau_{n'}(\varepsilon_{k'})\right). \tag{3.6}$$

Transforming the k' sum into an integral, one also obtains

$$\tau_n(\varepsilon_k) = \tau^0_n(\varepsilon_k)\left(1 + \sum_{n'} \int F^{n'}_n(\varepsilon_k,\varepsilon_{k'})\tau_{n'}(\varepsilon_{k'})d\varepsilon_{k'}\right) \tag{3.7}$$

with

$$F^{n'}_n(\varepsilon_k,\varepsilon_{k'}) = \frac{m^*}{4\pi^2}\int G_{n,n'}(k,k')\frac{f_{0,n'k'}(1-f_{0,n'k'})}{f_{0,nk}(1-f_{0,nk})}\frac{k'}{k}\cos(\theta)d\theta. \tag{3.8}$$

Note that the various matrix elements $F^{n'}_n(\varepsilon_k,\varepsilon_{k'})$ only require one angular integral and, therefore, a low computational demand. The remaining energy integral equation (3.7) may be transformed into a matrix inversion problem by limiting the energy integration range by a maximum value $\varepsilon_{\max}$ and then dividing the energy domain into N elementary steps $\Delta\varepsilon$, so that $\varepsilon_j = j\Delta\varepsilon$ and

$$\tau^0_{n,i} = \sum_{n',j}(\delta^{n'}_n \delta^j_i - \Delta\varepsilon\,\tau^0_n(\varepsilon_i)F^{n'}_n(\varepsilon_i,\varepsilon_j))\tau_{n',j} = \sum_{n',j} M^{n'}_n(i,j)\tau_{n',j}, \tag{3.9}$$

where each square $M^{n'}_n$ matrix is $N\times N$. The final solution of equation (3.9) is obtained as follows. The following vectors are defined

$$\tau = \begin{pmatrix} \tau_1(\varepsilon_j) \\ \tau_2(\varepsilon_j) \\ \text{etc.} \end{pmatrix} \quad \text{and} \quad \tau^0 = \begin{pmatrix} \tau^0_1(\varepsilon_j) \\ \tau^0_2(\varepsilon_j) \\ \text{etc.} \end{pmatrix}. \tag{3.10}$$

Thus, Eq. (3.9) transforms into a matrix equation

$$\begin{pmatrix} M^1_1(i,j) & M^2_1(i,j) & \text{etc.} \\ M^1_2(i,j) & M^2_2(i,j) & \text{etc.} \\ \text{etc.} & \text{etc.} & \text{etc.} \end{pmatrix} \times \begin{pmatrix} \tau_1(\varepsilon_i) \\ \tau_2(\varepsilon_i) \\ \text{etc.} \end{pmatrix} = \begin{pmatrix} \tau^0_1(\varepsilon_j) \\ \tau^0_2(\varepsilon_j) \\ \text{etc.} \end{pmatrix}. \tag{3.11}$$

The maximum $\varepsilon_{\max}$ value (i.e., the N value) must be chosen in order to get a convergent result (in our calculations $\varepsilon_{\max} = 7\omega_{\text{LO}}$). Then, the above matrix equation $\bar{\bar{M}}\times\bar{X} = \bar{V}$ is solved using standard numerical matrix inversion procedures.

IV. NUMERICAL RESULTS AND DISCUSSION

Usually, for the sake of simplicity in transport calculations, the wave functions needed for the evaluation of the various matrix elements are chosen under the form of trial analytical functions,[7,27,28] which, in practice, only allow the description of the first subband and prevent to consider exchange and correlation potentials. However, various self-consistent numerical approaches including Coulomb, exchange, and correlation potentials have been established in the past decades in order to obtain a true description of the energy states and their corresponding wave functions as for instance in Refs. 29–31 In the present work, in order to simulate the quantum well mobility and to check the effect of the carrier confinement on the various scattering mechanisms, we have determined numerically the energy states and their associated wave functions, adapting methods usually used in *ab initio* calculations to the establishment and the resolution of the envelop function equation. The Coulomb interaction and the exchange and correlation contributions,[32–34] as well as the Ben Daniel-Duke kinetic energy operator[35] accounting for the spatial dependence of the effective mass were introduced in the Kohn-Sham-like envelope equation. Our numerical method is based on the following assumption: Since the quantum well states are localized, it is assumed that their corresponding wave functions vanish at the extremities of a segment of length L in which the quantum well potential is imbedded. Thus, the wave functions may be expressed as a Fourier series of planes waves that are naturally defined by the segment length L. In this plane wave basis, the envelop function Kohn-Sham equation transforms into a matrix where the Coulomb as well as the exchange and correlation potentials are automatically calculated using the fast Fourier transform technique. The Kohn-Sham Hamiltonian matrix eigenelements are then numerically solved using an iterative procedure and their eigenvalues allow, finally, to calculate the full quantum well energy $E_T(L)$, which turns out to be a function of the parameter L. This last value L is chosen in order to minimize E_T. This variational procedure, already used in Refs. 36 and 37, allows us to get precise numerical results with a relatively low number of planes waves ($\sim$50 in the present one-dimensional localized case).

The numerical method described above is valid for any shape of quantum well binding potential. In the particular case of AlGaN/GaN quantum well, it is supposed that the quantum well arises because of an intrinsic positive charge σ, issuing from the spontaneous polarization and from the piezoelectric response of the strained AlGaN cap layer. This

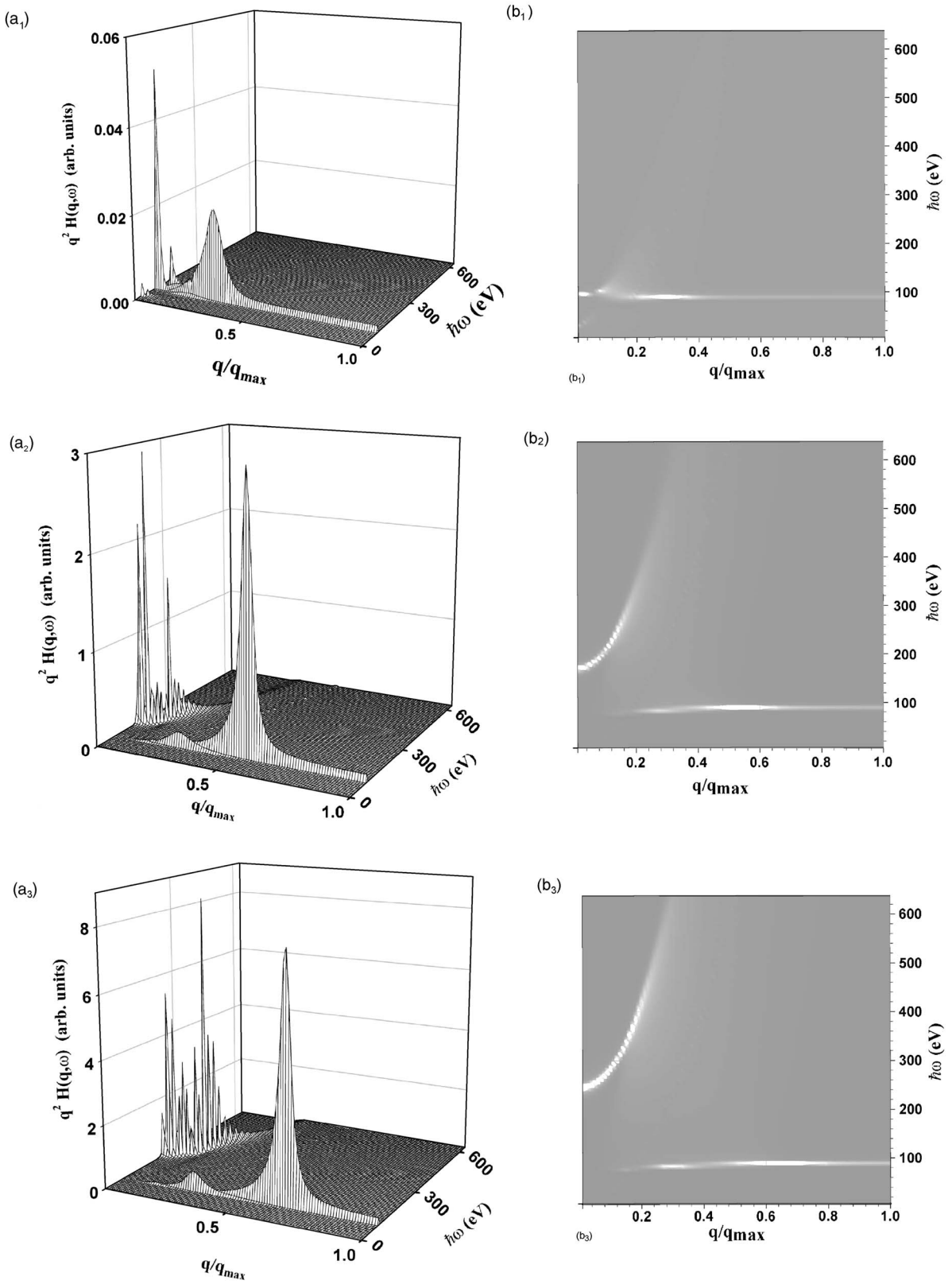

FIG. 1. Scattering strength map showing the function $H_{11}(q,\omega)$ (multiplied by q^2 in order to avoid too large values at small q) associated with hybrid bosons. The spectrum separates into a nondispersive phonon-like branch and a plasmon branch. (a_1) and (b_1) correspond to $n_s=2.10^{12}$ cm^{-2}; (a_2), (b_2) correspond to $n_S=1.2\ 10^{13}$ cm^{-2}; (a_3), (b_3) correspond to $n_S=2\ 10^{13}$ cm^{-2}.

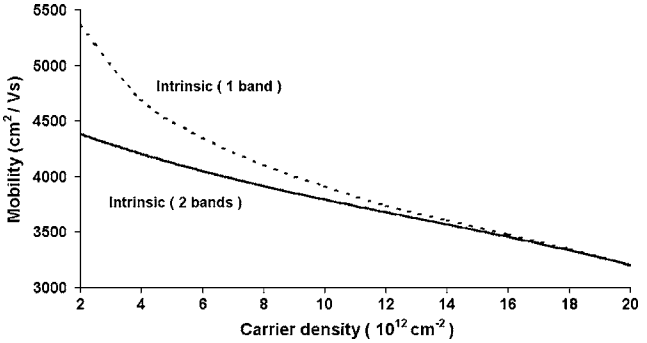

FIG. 2. Theoretical calculation of the room temperature intrinsic mobility versus carrier density in neutral triangular AlGaN/GaN quantum wells (dashed line: mobility calculated taking into account only the first subband; full line: mobility calculated taking into account the two first subbands).

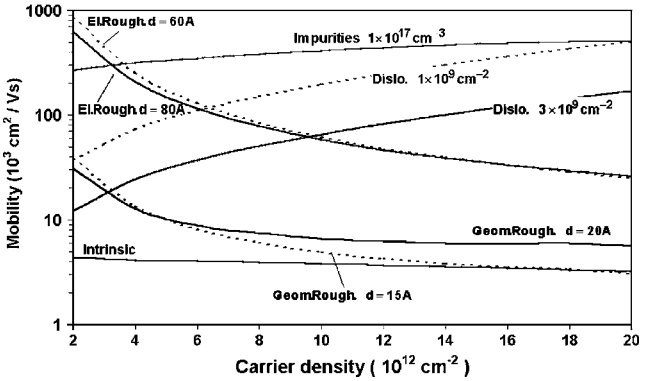

FIG. 3. Room temperature mobility versus carrier density limited by individual scattering mechanisms given for various parameters as indicated on the figure. The full lines correspond to the parameters chosen in the following for the calculation of total mobility.

charge is localized at the interface and creates an attractive potential given by

$$W_{\mathrm{QW}}(z) = \frac{2\pi\sigma}{\varepsilon_L}|z|. \tag{4.1}$$

Associated with the AlGaN/GaN band offset, such a bare potential creates an attractive triangular quantum well. In the present calculation, we have supposed that the electronic density n_s contained in the well is equal to σ, leading to a globally neutral quantum well. However other situations can be considered.

Making use of such wave functions, the scattering strength associated with hybrid particles could be numerically computed in the case of triangular AlGaN/GaN quantum wells. As an example, Fig. 1 shows, for various free carrier densities, the numerical computation of the function $H_{11}(q,\omega)$ whose general expression is given by

$$H_{n,n'}(q,\omega) = \mathrm{Im}\left\{ \sum_{m,m'} [\varepsilon^{-1}(q,\omega)]_{n',n}^{m',m} \times \int \frac{G^*_{n',n}(q'_z) G_{m',m}(q_z) e^{i(q_z - q'_z)z_0}}{q^2 + q_z^2} dq_z dq'_z \right\}. \tag{4.2}$$

The dielectric tensor components were numerically computed using (1.1), (2.17), and (2.18) with a damping phonon coefficient equal to $\gamma = 0.0035\omega_{\mathrm{LO}}$ (Refs. 26 and 38 and the plasmon damping frequency was set to $\alpha = 2/\langle\tau_B\rangle$ where $\langle\tau_B\rangle$ is the mean relaxation time.[39]

Figures $1(a_1)$–$1(a_3)$ and $1(b_1)$–$1(b_3)$, respectively, represent the 3D view and the top view for convenience. Figures $1(a_1)$ and $1(b_1)$ are obtained for a carrier density equal to 2×10^{12} cm^{-2}. The frequency spectrum is mainly made of a nondispersive optical phonon-like branch contribution. Nonetheless, a weak dispersive plasmon contribution starts to be visible. For lower densities the phonon and/or plasmon hybrid contribution to scattering becomes negligible and phonons alone should constitute the main scattering mechanisms, a situation that is expected, for instance, in the classical AlGaAs/GaAs quantum wells whose carrier densities are of the order of $\sim 10^{11}$ cm^{-2}. For larger densities the phonon and plasmon branch-like contribution and their coupling are clearly seen in Figs. $1(a_2)$ and $1(b_2)$ obtained for a carrier density equal to 1.2×10^{13} cm^{-2} and in Figs. $1(a_3)$ and $1(b_3)$ obtained for a carrier density equal to 2×10^{13} cm^{-2}. This behavior where plasmon and/or phonon hybrid particles scattering is no more negligible appears to be a particularity of AlGaN/GaN quantum wells capable of storing very high carrier densities.

Using the above numerical results, the intrinsic mobility could be determined and Fig. 2 exhibits the intrinsic mobility versus carrier density obtained at room temperature by combining the effect of polar phonon and/or plasmon hybrid scattering with the usual intrinsic scattering mechanisms associated with acoustic phonons (through the deformation potential and the piezoelectric coupling). This figure shows also the important role of intersubband transitions at low carrier densities (where more than one subband is noticeably occupied by electrons): the dashed line is obtained by neglecting the second subband, while the full line is obtained by taking into account the two first subbands of the quantum well. In any case, Fig. 2 shows a relatively important decrease of the room temperature mobility with increasing carrier densities that may be interpreted by the following arguments:

(i) An increasing carrier density obviously leads to a stronger carrier-carrier interaction (through the appearance of a more efficient plasmon contribution to scattering).

(ii) An increasing carrier density also leads to a stronger and stronger confinement of the quantum well wave functions resulting into a larger uncertainty of the q_z wave vector of the wave functions. Thus, more and more hybrid particles are involved in the scattering efficiency, as a consequence of the Heisenberg inequality.

(iii) The efficiency of the hybrid particle scattering is important at room temperatures, but it decreases at lower temperatures because of the presence of the Bose-Einstein statistics.

In order to point out the relative importance of the intrinsic scattering versus the other usual extrinsic scattering

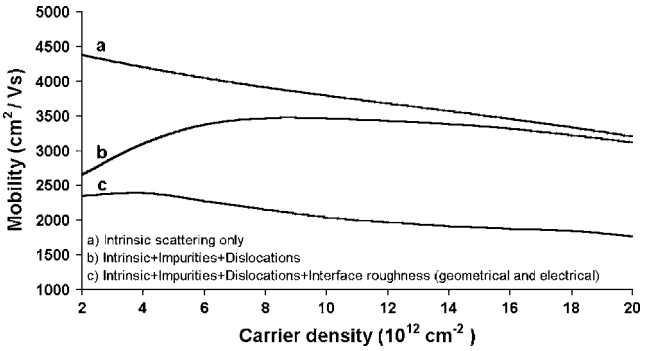

FIG. 4. Room temperature mobility versus carrier density resulting from the combination of extrinsic and intrinsic scattering centers: calculations are done using the set of parameters associated with full lines in Fig. 3 in order to reproduce the behavior of the mobility versus carrier density published in Ref. 41.

mechanisms, we have combined the effect of hybrid particles and acoustic phonons with the one of impurities, dislocations, and interface roughness in the relaxation times calculation. For that purpose, the following apply:

(i) impurities have been considered as uniformly distributed in the whole heterostructure with a density of 10^{17} cm^{-3}.

(ii) Threading dislocations have been considered acting through their possible linear charge (filling factor chosen as 0.3 and density as $1-3\times10^{9}$ cm^{-2}), although other scattering mechanisms can be associated with dislocations such as deformation potential, quantum box-like behavior, as it will be discussed in a following paper.

(iii) The interface geometrical roughness, resulting from the presence of islands at the AlGaN/GaN interface, has been introduced using the scattering potential already described in Ref. 9 in which the covering ratio has been set up to 25%, the island thickness to one monolayer and the correlation length either to 15 A or to 20 A.

(iv) The so called "electrical roughness," associated with the fact that the interface charge may not be uniform because of various elastic relaxation mechanisms (including thus, in a phenomenological way, the possible presence of misfit dislocation tangles, interface cracks, alloy reordering, etc.), has as well been introduced in our calculation with a covering ratio set up to 25%, the average local charge variation to 25%, and the correlation length either to 60 A or to 80 A.

The individual effects of each extrinsic scattering mechanism on the mobility are represented in Fig. 3, as well as the one of intrinsic scattering (hybrid optical phonon and/or plasmon particles and acoustic phonons). This figure clearly demonstrates that intrinsic scattering mechanisms are, at room temperature and at high carrier densities, the most efficient scattering centers. As it was already shown in Ref. 9, impurities and dislocation mainly act at low carrier densities because of weaker screening effects, while the interface geometrical and electrical roughness efficiency increases with the carrier density. Thus, the total mobility versus carrier density resulting from the simultaneous action of extrinsic and intrinsic scattering mechanisms goes through a maximum, as it is experimentally observed for instance in Ref. 40, but whose theoretical position obviously depends on the various parameters introduced in the calculation (dislocation densities and dislocation linear charge, correlation lengths and covering ratio for the interface roughnes, etc.). Such a simultaneous effect of the various scattering centers on the total mobility is visible in Fig. 4 (c): here, the calculations are done with a choice of parameters allowing us to reproduce, at best, the recent experimental results shown in Ref. 41 for which the maximum mobility versus carrier density occurs at relatively low carrier density.

ACKNOWLEDGMENTS

This work has been supported by the European Spatial Agency in the frame of ATHENA (ESTEC-Contract No. 14205/00/NL/PA). The authors thank M. Germain for valuable discussions.

[1] F. Bernardini, V. Fiorentini, and D. Vanderbilt, Phys. Rev. B **56**, R10024 (1997).
[2] I. P. Smorchkova, C. R. Elsaas, J. P. Ibbetson, R. Vetury, B. Heying, P. T. Fini, E. Haus, S. P. DenBaars, J. S. Speck, and U. K. Mishra, J. Appl. Phys. **86**, 4520 (1999).
[3] J. A. Garrido, J. L. Sanchez-Rojas, A. Jiménez, E. Munoz, F. Omnes, and P. Gibart, Appl. Phys. Lett. **75**, 2407 (1999).
[4] J. P. Ibbetson, P. T. Fini, K. D. Ness, S. P. DenBaars, J. S. Speck, and U. K. Mishra, Appl. Phys. Lett. **77**, 250 (2000).
[5] B. K. Ridley, O. Ambarer, and L. Eastman, Semicond. Sci. Technol. **15**, 270 (2000).
[6] O. Ambarer, B. Foutz, J. Smart, J. R. Shealy, N. G. Weimann, K. Chu, A. J. Sierakowski, W. J. Schaff, L. F. Eastman, R. Dimitrov, A. Mitcell, and M. Stutzmann, J. Appl. Phys. **87**, 334 (2000).
[7] Z. Bougrioua, J-L. Farvacque, I. Moerman, and F. Carosella, Phys. Status Solidi B **228**, 625 (2001).
[8] J-L. Farvacque, Z. Bougrioua, F. Carosella, and I. Moerman, J. Phys.: Condens. Matter **14**, 13319 (2002).
[9] J-L. Farvacque and Z. Bougrioua, Phys. Rev. B **68**, 035335 (2003).
[10] Z. Bougrioua (private communication).
[11] I. P. Smorchkova, L. Chen, T. Mates, L. Shen, S. Heikman, B. Moran, S. Keller, S. P. DenBaars, J. S. Speck, and U. K. Mishra, J. Appl. Phys. **90**, 5196 (2001).
[12] J. C. Garland and R. Bowers, Phys. Rev. Lett. **21**, 1007 (1968).
[13] C. Hodges, H. Smith, and J. W. Wilkins, Phys. Rev. B **4**, 302 (1971).
[14] W. E. Laurence and J. W. Wilkins, Phys. Rev. B **7**, 2317 (1973).
[15] M. Kaveh and N. Wiser, J. Phys. F: Met. Phys. **10**, L37 (1980).
[16] S. De Gennaro and A. Rettori, J. Phys. F: Met. Phys. **14**, L237 (1984).
[17] D. Movshovitz and N. Wiser, J. Phys. F: Met. Phys. **17**, 985 (1987).

[18] B. E. Sernelius and Söderström, J. Phys.: Condens. Matter **3**, 8425 (1991).
[19] B. K. Ridley, *Quantum Processes in Semiconductors* (Clarendon Press, Oxford, UK, 1993).
[20] M. Born and K. Huang, *The Dynamical Theory of Crystal Lattices* (Clarendon Press, Oxford, UK, 1956).
[21] R. W. Stimets and B. Lax, Phys. Rev. B **1**, 4720 (1970).
[22] J. Lindhard and K. Dan. Vidensk, K. Dan. Vidensk. Selsk. Mat. Fys. Medd. **28**, 8 (1954).
[23] B. B. Varga, Phys. Rev. **137**, A1896 (1965).
[24] M. E. Kim, A. Das, and S. D. Senturia, Phys. Rev. B **18**, 6890 (1978).
[25] J-L. Farvacque, Phys. Rev. B **67**, 195324 (2003).
[26] D. R. Anderson, M. Babiker, C. R. Bennett, and M. I. J. Porbert, Physica E (Amsterdam) **17**, 272 (2003).
[27] T. Ando, A. B. Fowler, and E. Stern, Rev. Mod. Phys. **54**, 437 (1982).
[28] B. K. Ridley, B. E. Foutz, and L. F. Eastman, Phys. Rev. B **61**, 16862 (2000).
[29] J. Hautman and L. M. Sander, Phys. Rev. B **30**, 7000 (1984).
[30] J. Hautman and L. M. Sander, Phys. Rev. B **32**, 980 (1985).
[31] M. P. Stopa and S. Das Sarma, Phys. Rev. B **47**, 2122 (1993).
[32] D. M. Ceperley and B. J. Alder, Phys. Rev. Lett. **45**, 566 (1980).
[33] J. P. Perdew and A. Zunger, Phys. Rev. B **23**, 5048 (1981).
[34] S. Nagaraja, P. Matagne, V-Y Thean, J-P. Leburton, Y. H. Kim, and R. M. Martin, Phys. Rev. B **56**, 15752 (1997).
[35] D. J. BenDaniel and C. B. Duke, Phys. Rev. **152**, 683 (1966).
[36] D. Brinkmann, Diplomarbeit, University Grenoble, 1995.
[37] J-L. Farvacque and P. François, Phys. Status Solidi B **223**, 635 (2001).
[38] B. K. Ridley, J. Phys.: Condens. Matter **8**, L511 (1996).
[39] J. R. Meyer and F. J. Bartoli, Phys. Rev. B **28**, 915 (1983).
[40] J. Antoszewski, M. Gracey, J. M. Dell, L. Faraone, T. A. Fisher, G. Parish, Y. F. Wu, and U. K. Mishra, J. Appl. Phys. **87**, 3900 (2000).
[41] A. Wells, M. J. Uren, R. S. Balmer, K. J. Nash, T. Martin, and M. Missous, Phys. Status Solidi A **202**, 812 (2005).